CHEMISTRY LETTERS, pp. 1243-1246, 1988. 

# Digital Simulation of Normal Pulse Polarographic Adsorption Waves of Methyl Viologen

Katsuyoshi KOBAYASHI
Department of Electrochemistry, Yokohama National University,
156, Tokiwadai, Hodogaya-ku, Yokohama 240

Digital simulations of the normal pulse polarographic adsorption waves of the nernstian redox species obeying the Frumkin type Flory-Huggins isotherm interpret the unusual electrochemical behavior of methyl viologen. An orientation change of the adsorbed reductant causes a marked positive shift of adsorption waves.

In the previous work,[1] we have reported by using various voltammetric techniques that the several unusual adsorption phenomena which are observed in the normal pulse polarogram (NPP) of 1,1'-dimethyl-4,4'-dipyridinium dichloride (methyl viologen, MV) are caused by the changes in both the orientation and the interaction between the adsorbed $MV^{+\cdot}$ (reduced form of MV) molecules on the mercury electrode. It is interesting to interpret the adsorption behavior of MV by analysing mathematically the electrochemical system where both the orientation and interaction of the adsorbed species change.

The simulations of NPP reported by Flanagan et al.[2] and Lovric[3] are based on the assumption that the oxidized (Ox) and the reduced (Rd) species are each adsorbed on the electrode independently. Therefore, their simulations are inapplicable to the electrochemical system in which both Ox and Rd are adsorbed strongly on the electrode at relatively high concentrations of redox species where sharp prewaves or postwaves often appear. In the present simulation, in order to consider the simultaneous adsorption of Ox and Rd, the change of the area occupied by an adsorbed molecule due to the orientation change of adsorbed molecules, and the interactions between adsorbed redox molecules, the Frumkin type Flory-Huggins isotherm was postulated as the adsorption isotherm:[4]

$$B_O C_O = [\Theta_O/N_O(1 - \Theta_O - \Theta_R)^{N_O}]\exp(N_O A_O \Theta_O + N_O A_{OR}\Theta_R) \qquad (1)$$

and

$$B_R C_R = [\Theta_R/N_R(1 - \Theta_O - \Theta_R)^{N_R}]\exp(N_R A_R \Theta_R + N_R A_{OR}\Theta_O), \qquad (2)$$

where $B_O$ and $B_R$ are the adsorption coefficients of Ox and Rd ($B_O = K_O/\Gamma_{O,m}$ and $B_R = K_R/\Gamma_{R,m}$, $K_O$ and $K_R$ are the Henry constants of Ox and Rd, $\Gamma_{O,m}$ and $\Gamma_{R,m}$ the maximum values of $\Gamma_O$ and $\Gamma_R$, $\Gamma_O$ and $\Gamma_R$ the surface concentrations of Ox and Rd on the electrode), $C_O$ and $C_R$ the concentrations of Ox and Rd in the solution at the vicinity of the electrode, $\Theta_O$ and $\Theta_R$ the coverages of Ox and Rd ($\Theta_O = \Gamma_O/\Gamma_{O,m}$ and $\Theta_R = \Gamma_R/\Gamma_{R,m}$), $N_O$ and $N_R$ the number of molecules of water (or clusters of water molecules) displaced by one molecule of Ox and Rd, $A_O$, $A_R$, and $A_{OR}$ the constants of interaction between molecules of Ox, molecules of Rd, and molecules of Ox and Rd, respectively. It was assumed that the rates of adsorption-desorption processes were sufficiently fast, and $K_O$, $K_R$, $\Gamma_{O,m}$, $\Gamma_{R,m}$, $N_O$, $N_R$, $A_O$, $A_R$, and $A_{OR}$ were independent of potential ($E$). The electrode reaction was assumed to be reversible for both Ox and Rd soluble in the solution. Initially, only Ox is present in the solution ($C_O$*, the bulk concentration). The values of $C_O$, $C_R$, $\Theta_O$, and $\Theta_R$ at $E$ can be calculated from Eqs. 1 and 2, and the Nernst equation by using $C_O$*. $A_{OR}$ was assumed to be negligible relative to $A_O$ and $A_R$.[5] Then, the combination of Eqs. 1 and 2 leads to

$$1 - \Theta_R - f(\Theta_R) - \{[f(\Theta_R)/N_O B_O C_O]\exp[N_O A_O f(\Theta_R)]\}^{1/N_O} = 0, \qquad (3)$$

where

$$f(\Theta_R) = 1 - \Theta_R - [(\Theta_R/N_R B_R C_R)\exp(N_R A_R \Theta_R)]^{1/N_R}. \qquad (4)$$

The Brent method was applied to calculate $\Theta_R$ from Eq. 3 because more than one so-

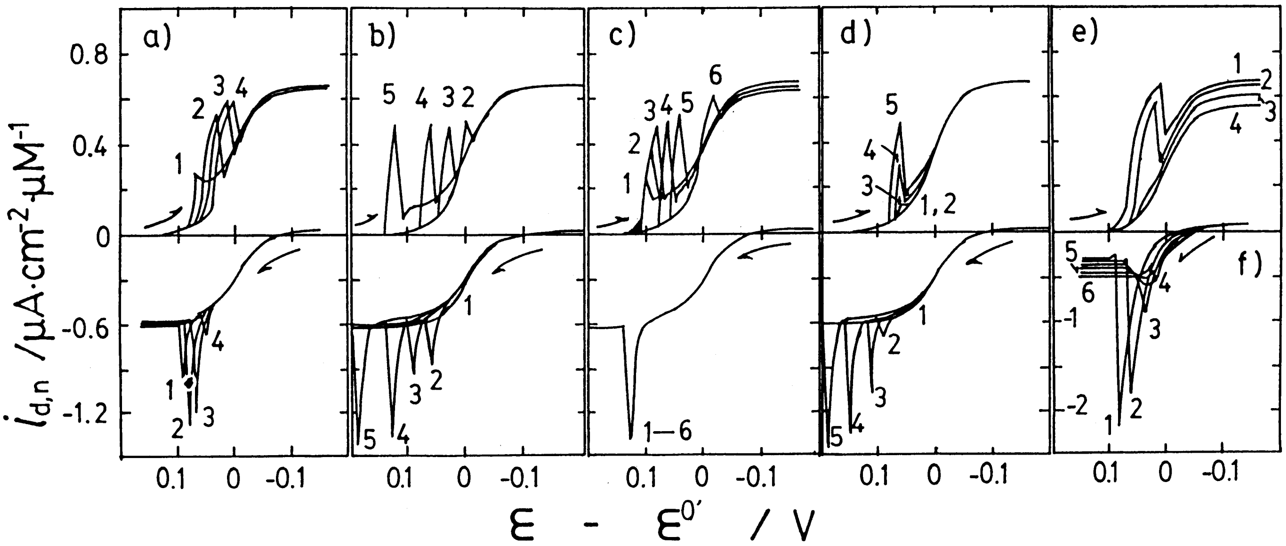


Fig. 1. Effects of a) $K_O$, b) $K_R$, c) $A_O$, d) $A_R$, e) $N_O$, and f) $N_O$ and $N_R$ on the simulated NPP.

| | a) | b) | c) | d) | e) | f) |
|---|---|---|---|---|---|---|
| $C_O$* /mM[6] | 1 | 1 | 1 | 1 | 1 | 0.1 |
| $K_O$ /cm | v1 | $10^{-4}$ | $10^{-4}$ | $10^{-4}$ | $2\times10^{-3}$ | $10^{-4}$ |
| $K_R$ /cm | $10^{-3}$ | v2 | $10^{-3}$ | $10^{-3}$ | $10^{-3}$ | $10^{-3}$ |
| $A_O$ | 0.5 | -1 | v3 | -1.6 | 0.5 | -1 |
| $A_R$ | -2.5 | -2 | -2 | v4 | -2.5 | -2 |
| $N_O$ | 4 | 16 | 16 | 16 | v5 | v6 |
| $N_R$ | 2 | 4 | 4 | 4 | 2 | v7 |
| $\Gamma_{O,m}$ /mol·cm$^{-2}$ | $2\times10^{-10}$ | $10^{-10}$ | $10^{-10}$ | $10^{-10}$ | v8 | $2\times10^{-10}$ |
| $\Gamma_{R,m}$ /mol·cm$^{-2}$ | $4\times10^{-10}$ | $4\times10^{-10}$ | $4\times10^{-10}$ | $4\times10^{-10}$ | $4\times10^{-10}$ | $4\times10^{-10}$ |

v1: 1) $10^{-4}$, 2) $10^{-3}$, 3) $3\times10^{-3}$, 4) $10^{-2}$. v2: 1) $10^{-5}$, 2) $10^{-4}$, 3) $3\times10^{-4}$, 4) $10^{-3}$, 5) $10^{-2}$. v3: 1) 1, 2) 0.5, 3) 0, 4) -1, 5) -1.2, 6) -1.6. v4: 1) 1, 2) 0.5, 3) 0, 4) -1, 5) -2. v5: 1) 8, 2) 4, 3) 2, 4) 1. v6: 1) 8, 2) 6, 3) 5, 4) 4, 5) 3, 6) 2. v7: 1) 4, 2) 3, 3) 2.5, 4) 2, 5) 1.5, 6) 1. v8: 1) $10^{-10}$, 2) $2\times10^{-10}$, 3) $4\times10^{-10}$, 4) $8\times10^{-10}$. Other parameters: $t_d$[6]=2 s, $t_s$[6]=30 ms, $D_O=D_R$[7]=$4.4\times10^{-6}$ cm$^2$/s, $m_{Hg}$[8]=1.34 mg/s. $E^{0'}$: formal potential, $i_{d,n}$: normalized current density.

lution was often obtained at $\mathcal{E}$ (e.g. sigmoid type isotherm). The most stable and current-determining solution was assumed to be such $\Theta_R$ that $|d(\Theta_R)/d\mathcal{E}|$ was the least.[4] The concentration profile in the diffusion layer at time $t$ was calculated by modifying Flanagan's program.[2] All calculations in the present simulations were carried out on a computer, Hitac M 240H (Hitachi Co.). All listing of the simulation program is available on request.

Figures 1a, 1b, 1c, 1d, 1e, and 1f show the effects of $K_O$, $K_R$, $A_O$, $A_R$, $N_O$, and both $N_O$ and $N_R$ on the simulated NPP, respectively. Both the decrease in $K_O$ and the increase in $K_R$ led to the positive shift of the peak potential ($\mathcal{E}_p$). As $A_O$ changed from attractive to repulsive in the forward scan, the cathodic peak potential shifted toward positive potentials and tended to approach the constant potential with the more repulsive $A_O$. In the reverse scan, however, the change of $A_O$ gave no effect on NPP. The more attractive $A_R$ caused both the appearance of the prewave in the forward scan and the positive shift of the anodic peak potential ($\mathcal{E}_{p,a}$) in the reverse scan. As $N_O$ became large keeping $N_R$ constant, the adsorption peak appeared. The increase in both $N_O$ and $N_R$ keeping the ratios of $N_O/N_R$ constant, caused both the increase in the peak current ($i_p$) and the positive shift of $\mathcal{E}_{p,a}$. Figure 2 shows both the concentration dependences of $\mathcal{E}_{1/2,s}$ (the half-wave potential of single wave) and $\mathcal{E}_p$ in the forward scan of the measured[1] and simulated NPP. Table 1 shows ratios of measured[1] to calculated values of both $i_l$ and $i_p$ in the reverse scan of NPP. As are shown in Table 1, the $i_l$ and $i_p$ which were calculated with simulation 1 agreed with the $i_l$ and $i_p$ which were measured in the reverse scan of NPP. As are shown in Fig. 2, however, the $\mathcal{E}_{1/2,s}$ calculated with simulation 1 was almost constant with concentrations, independent of $t_s$, and very different from the measured $\mathcal{E}_{1/2,s}$, whereas the calculated $\mathcal{E}_p$ with simulation 1 agreed with the measured $\mathcal{E}_p$. The slow positive shift of the measured $\mathcal{E}_p$ from $\mathcal{E}^{0'}$ with an increase in the concentration at concentrations higher than 0.5 mM can be simulated with both a strongly attractive $A_R$ and not too large $K_R$ ($K_R$ = $10^{-4}$–$10^{-2}$cm). The abrupt positive shift of the measured $\mathcal{E}_{1/2,s}$ from $\mathcal{E}^{0'}$ with a decrease in the concentration and the dependence of $\mathcal{E}_{1/2,s}$ on $t_s$ at concentrations lower than 0.5 mM can

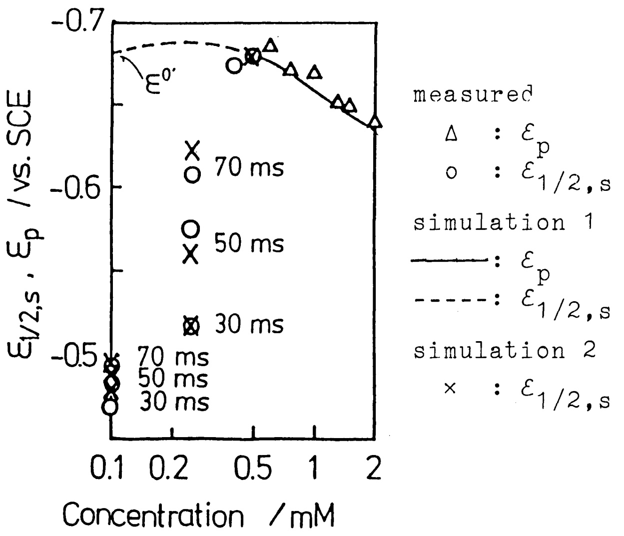


Fig. 2. Concentration dependences of $\mathcal{E}_{1/2,s}$ and $\mathcal{E}_p$ in the forward scan of NPP. Other parameters are given in the caption of Fig. 1.

| | simulation 1 | simulation 2 |
|---|---|---|
| $C_O$* /mM | 0.1–2 | 0.1–0.5 |
| $K_O$ /cm | $2\times10^{-3}$ | $2\times10^{-3}$ |
| $K_R$ /cm | $8\times10^{-4}$ | 4 |
| $A_O$ | 0.5 | 0.5 |
| $A_R$ | -2.5 | -0.5 |
| $N_O$ | 4 | 4 |
| $N_R$ | 2 | 3.2 |
| $\Gamma_{O,m}$ /mol·cm$^{-2}$ | $2\times10^{-10}$ | $2\times10^{-10}$ |
| $\Gamma_{R,m}$ /mol·cm$^{-2}$ | $4\times10^{-10}$ | $2.5\times10^{-10}$ |
| orientation of Rd | vertical | flat |

Table 1. Ratios of measured to calculated values of both $i_l$[a)] and $i_p$ in the reverse scan of NPP[b)]

| Concentration /mM | 2 | 1 | 0.75 | 0.25 | 0.1 |
|---|---|---|---|---|---|
| $(i_{l,m}/i_{l,c})$[c)] | 1.1 | 0.97 | 1.0 | 0.96 | 0.95 |
| $(i_{p,m}/i_{p,c})$[c)] | 1.2 | 0.89 | 0.73 | 0.83 | 1.7 |

a) $i_l$ is the limiting current of NPP. b) Simulation parameters are the same as those for simulation 1 in Fig. 2. $t_s$ = 30 ms. c) $i_{l,m}$ and $i_{p,m}$ are $i_l$ and $i_p$ of the measured NPP,[1)] and $i_{l,c}$ and $i_{p,c}$ are $i_l$ and $i_p$ of the simulated NPP.

be simulated with both large $K_R$ ($K_R$ > 0.1) and not too attractive $A_R$ ($A_R$ > -2). The marked changes in both $K_R$ and $A_R$ with concentrations can be interpreted with considering the reorientation of adsorbed Rd molecules from vertical to flat. $i_l$ and $E_{1/2,s}$ of NPP which were measured in the forward scan at $C_O^* < 0.5$ mM could be simulated on simulation 2. It has been evaluated in the MV system that $\Gamma_{O,m} = 2.0 \times 10^{-10}$ mol·cm$^{-2}$, $\Gamma_{R,m} = 4.4 \times 10^{-10}$ mol·cm$^{-2}$,[1)] $N_O$ = 3.4, and $N_R$ = 1.5–3.4.[1,5)] It has been reported that $A_O$ = 0.5 in the flat orientation and $A_R$ = -0.5 in the vertical orientation for the pyridine system,[9)] and $A_O$ = 0, $A_R$ = -5.8,[10)] $K_O = 3 \times 10^{-4}$ cm, and $K_R$ = 0.3 cm[11)] (even $K_R$ = 4 cm[10)]) for the system of Methylene Blue. The adsorption coefficient can increase by $10^3$–$10^4$ times due to π-electron interaction.[12)] It is estimated that the $MV^{+\cdot}$ molecules with two pyridyl rings where a radical was added with one-electron reduction can strongly adsorb on the electrode by π-electron interaction in the flat orientation, and can interact attractively more than pyridine molecules in the vertical orientation. The values of parameters on simulation 1 and simulation 2 are plausible. The peculiar polarographic adsorption behavior of MV is probably caused by the reorientation of adsorbed $MV^{+\cdot}$.

The author would like to thank Professor Katsumi Niki, Yokohama National University, for helpful discussions.

References

1) K. Kobayashi, F. Fujisaki, T. Yoshimine, and K. Niki, Bull. Chem. Soc. Jpn., 59, 3715 (1986).
2) J. B. Flanagan, K. Takahashi, and F. C. Anson, J. Electroanal. Chem. Interfacial Electrochem., 85, 257 (1977).
3) M. Lovric, J. Electroanal. Chem. Interfacial Electrochem., 197, 49 (1986).
4) E. Laviron, J. Electroanal. Chem. Interfacial Electrochem., 63, 245 (1975).
5) J. M. Parry and R. Parsons, J. Electrochem. Soc., 113, 992 (1966).
6) 1 M = 1 mol·dm$^{-3}$. $t_d$ and $t_s$ are a drop time and a sampling time of NPP.
7) $D_O$ and $D_R$ (diffusion coefficients of Ox and Rd) were evaluated by NPP of MV.
8) $\ell_{Hg}$ is the rate of mercury flow from the dropping mercury electrode.
9) B. B. Damaskin, A. A. Sulvila, S. Ya. Vasina, and A. I. Fedorova, Sov. Electrochem., 3, 729 (1967).
10) G. Piccardi, F. Pergola, M. L. Foresti, and R. Guidelli, J. Electroanal. Chem. Interfacial Electrochem., 84, 235 (1977).
11) R. H. Wopschall and I. Shain, Anal. Chem., 39, 1527 (1967).
12) E. Blomgren, J. O'M. Bockris, and C. Jesch, J. Electrochem. Soc., 65, 2000 (1961).

(Received January 14, 1988)